8690 *Inorg. Chem.* **2010**, *49*, 8690–8698
DOI: 10.1021/ic902547t

Inorganic Chemistry
Article

Structural Characterization and Antimicrobial Activity of the Zn(II) Complex with P113 (Demegen), a Derivative of Histatin 5

Elena Porciatti,[†] Marina Milenković,[‡] Elena Gaggelli,[†] Gianni Valensin,[†] Henryk Kozlowski,[§] Wojciech Kamysz,[∥] and Daniela Valensin*[,†]

[†]*Department of Chemistry, University of Siena, via Aldo Moro, 53-100 Siena, Italy,*
[‡]*Faculty of Pharmacy, University of Belgrade, Vojvode Stepe 450, Belgrade, Serbia,*
[§]*Faculty of Chemistry, University of Wrocław F. Joliot-Curie 14, 50-383 Wrocław, Poland, and*
[∥]*Department of Inorganic Chemistry, Faculty of Pharmacy, Medical University of Gdańsk, Al. Gen. Hallera 107, 80-416 Gdańsk, Poland*

Received December 21, 2009

Zinc binding to P113 (or demegen), a 12 amino acid (AKRHHGYKRKFH-NH_2) fragment of histatin 5, was investigated by means of NMR and CD techniques, yielding delineation of the metal binding site and the 3D structure of the complex in water and in DMSO as well. The three His imidazole and the N-terminus nitrogens were found to act as the zinc coordinating atoms. A comparison with the previously reported Cu(II)-P113 complex disclosed that the two structures were rather diverse, in spite of an identical donor set. The two complexes were also tested for their antimicrobial activity *in vitro* against seven bacteria and two yeast strains: a minor activity of both complexes vs that of free ligand was given evidence, suggesting both metal ions may possibly play a negative role *in vivo*.

Introduction

Histatins are a group of small, histidine-rich cationic peptides secreted into the saliva by human parotid and submandibular−sublingual glands.[1] Histatins are known to display antimicrobial activity and to exhibit fungicidal activity against several *Candida* species, *Saccharomyces cerevisiae*, and *Cryptococcus neoformans*.[2,3] The maximum level of activity is observed for Histatin 5 (Hsn-5) (DSHAKRHHGYKRKFHEKHHSHRGY) against *Candida albicans*.

P113 (also called Demegen) is a C-terminus amidated Hsn-5 derivative (Hsn-5_{4-15}, AKRHHGYKRKFH-NH_2), that, like other histatins, is active against clinically important microorganisms such as *streptococci*, *staphylococci*, *Pseudomonas aeruginosa*, and *Candida albicans*.[4−6]

Previous investigations of Hsn-5 activity have pointed out a major role played by the two adjacent histidines (His-18 and His-19), such that substitution with alanine resulted into an 8- to 20-fold reduction in activity.[7] On the contrary, the antimicrobial activity of P113 is not affected by His substitution[4] but, rather, by replacing all four cationic residues (Lys-2, Arg-3, Arg-9, and Lys-10) with glutamine.[4]

Since both Hsn-5 and P113 sequences embody several potential metal binding sites, metal ions were suggested to eventually help or inhibit antimicrobial activities. Early studies were revealing for a specific action of Zn(II) due to the occurrence of the HExxH sequence, a recognized zinc-binding motif in many proteins.[8] Zn(II) was indeed shown to selectively induce the Hsn-5 property of aggregating and fusing negatively charged small unilamellar vesicles.[9] A significant Zn(II)-related enhancement of the antimicrobial activity of Hsn-5 against *E. faecalis* was also demonstrated.[10]

The formation of high affinity complexes between Cu(II) or Ni(II) or, to a lesser extent, Zn(II) and Histatins was assessed by electrospray ionization mass spectrometry (ESI-MS) and circular dichroism spectroscopy (CD).[11] Isothermal

*To whom correspondence should be addressed. E-mail: valensindan@unisi.it.

(1) Ahmad, M.; Piludu, M.; Oppenheim, F. G.; Helmerhorst, E. J.; Hand, A. R. *J. Histochem. Cytochem.* **2004**, *52*, 361–370.
(2) Driscoll, J.; Duan, C.; Zuo, Y.; Xu, T.; Troxler, R.; Oppenheim, F. G. *Gene* **1996**, *177*, 29–34.
(3) Helmerhorst, E. J.; Reijnders, I. M.; van't Hof, W.; Simoons-Smit, I.; Veerman, E. C.; Amerongen, A. V. *Antimicrob. Agents Chemother.* **1999**, *43*, 702–704.
(4) Rothstein, D. M.; Spacciapoli, P.; Tran, L. T.; Xu, T.; Roberts, F. D.; Dalla Serra, M.; Buxton, D. K.; Oppenheim, F. G.; Friden., P. *Antimicrob. Agents Chemother.* **2001**, *45*, 1367–1373.
(5) Sajjan, U. S.; Tran, L. T.; Sole, N.; Rovaldi, C.; Akiyama, A.; Friden, P. M.; Forstner, J. F.; Rothstein, D. M. *Antimicrob. Agents Chemother.* **2001**, *45*, 3437–3444.
(6) Sugiyama, K. *Experientia* **1993**, *49*, 1095–1097.
(7) Tsai, H.; Bobek, L. A. *Antimicrob. Agents Chemother.* **1997**, *41*, 2224–2228.
(8) Bode, W.; Gomis-Ruth, F. X.; Stöckler, W. *FEBS Lett.* **1993**, *331*, 134–140.
(9) Melino, S.; Rufini, S.; Sette, M.; Morero, R.; Grottesi, A.; Paci, M.; Petruzzelli, R. *Biochemistry* **1999**, *38*, 9626–33.
(10) Rydengård, V.; Andersson Nordahl, E.; Schmidtchen, A. *FEBS J.* **2006**, *273*, 2399–406.

Published on Web 09/03/2010

titration calorimetry yielded the binding constants at 1×10^5 M^{-1} and 3×10^7 M^{-1} for zinc− and copper−histatins, respectively.[12] The Zn(II) and Cu(II) binding sites of Hsn-5 were characterized by looking at metal-induced changes in NMR spectra:[13] it resulted that zinc binding involves His-15 within the −HExxH− zinc binding motif, and that copper binding occurs at the N-terminal DSH−, ATCUN motif.

As for P113, the stability constants, stoichiometry, and structures of the complexes formed by Cu(II) were characterized by potentiometric and spectroscopic (UV−vis, CD, EPR, NMR) measurements:[14] consideration of P113 and three mutants allowed demonstration of the His−His pair and the N-terminus making P113 a very attractive copper ligand.[14]

In the present study, the zinc binding abilities of P113 were investigated by using NMR and CD spectroscopy, and the antimicrobial activities of the Cu(II)− and Zn(II)−P113 complexes were assessed with the aim of shedding light on the eventual role played by these metal ions.

Experimental Section

Peptide Synthesis. P113 (AKRHHGYKRKFH-NH_2) and its N-acetylated parent peptide (AcP113) were synthesized manually using the solid-phase method on polystyrene AM-RAM resin (0.66 mmol/g; Rapp Polymere, Germany) using 9-fluorenylmethoxycarbonyl (Fmoc) chemistry.[15] The peptides were synthesized using the following procedure: (i) 5 and 15 min deprotection steps using 20% piperidine in dimethylformamide (DMF) in the presence of 1% Triton were used. (ii) The coupling reactions were carried out with the protected amino acid diluted in a mixture of DMF/N-methyl-2-pyrrolidone (NMP; 1:1, v/v) in the presence of 1% Triton using diisopropylcarbodiimide (DIC) as the coupling reagent in the presence of 1-hydroxybenzotriazole (HOBt; Fmoc-AA/DIC/HOBt, 1:1:1) for 2 h. The completeness of each coupling reaction was monitored by the chloranil test.[16] The peptides were cleaved from the solid support by trifluoroacetic acid (TFA) in the presence of water (2.5%) and triisopropylsilane (2.5%) as scavengers. The cleaved peptides were precipitated with diethyl ether and purified using high-performance liquid chromatography (HPLC) on a Knauer two-pump system with a Kromasil 10 × 250 mm (5 μm particle diameters, 100 Å pore size) C8 column with a flow rate of 5 mL/min, and absorbance at 226 nm. The peptides were analyzed using matrix-assisted laser desorption ionization-time-of-flight mass spectrometry (MALDI-TOF).

NMR Measurements. P113 and AcP113 samples were prepared by dissolving the powders either in H_2O/D_2O (9:1) or in TFE/D_2O (9:1) mixtures or in 100% DMSO-d_6. In the last case, peptides were first dissolved in H_2O, and the pH was adjusted at 7.0. Then, the samples were freeze-dried and dissolved in DMSO-d_6. Peptide concentrations in the range 0.5−2.0 mM were used. The 1D ^{1}H spectra were recorded at different temperatures. For the samples in DMSO-d_6, T = 318 K was chosen; whereas T = 278 K was used to analyze structural features in aqueous solutions. NMR measurements were performed either at 14.1 T with a Bruker Avance 600 MHz or at 9.4 T with a Bruker AMX 400 MHz spectrometer at controlled temperatures (±0.2 K) using a TBI (Triple Broadband Inverse) or BBI (Broadband Inverse) probe. Water suppression was achieved either by presaturation or by the excitation sculpting method.[17] Proton and carbon resonance assignment was accomplished through TOCSY, NOESY, ROESY, and HSQC standard experiments. TOCSY spectra were obtained using the MLEV-17 pulse sequence with a mixing time of 75 ms. NOESY and ROESY spectra were obtained at different values of the mixing time to optimize the best one. Spectra processing was performed on a Silicon Graphics O2 workstation using the XWINNMR 3.6 software.

CD Measurements. CD spectra were acquired on a Jasco spectropolarimeter at 298 K. A cell with a 0.1 cm path length was used for spectra recorded between 190 and 250 nm with sampling points every 1 nm. Four scans were collected for every sample with a scan speed of 20 nm/min and a bandwidth of 1 nm. Baseline spectra were subtracted from each spectrum, and data were smoothed with the Savitzky−Golay method.[18] Data were processed using the Origin 5.0 spread sheet/graph package. The direct CD measurements (θ, in millidegrees) were converted to mean residue molar ellipticity, using the relationship mean residue $\Delta\varepsilon = \theta/(33\,000 \times c \times l \times$ number of residue).

Structure Determination. For all of the investigated peptides, the intensities of NOESY cross-peaks, referenced to cross-peaks of proton pairs at fixed distances, were converted into proton−proton distance constraints.

The conformations of the metal complexes were obtained by using the distance sets determined from the volume of the cross-peaks of the NOESY spectra by means of the following relationship:

$$r_{ij} = r_{\mathrm{ref}} \sqrt[6]{\frac{I_{\mathrm{ref}}}{I_{ij}}}$$

where r_{ij} is the distance among the two correlated protons, r_{ref} is a reference distance, I_{ref} is the integral of the reference peak, and I_{ij} is the integral of the observed cross-peak.

The obtained distance restraints, together with those estimated for the metal coordination sphere, were used to build a pseudopotential energy for a restrained simulated annealing (SA) calculation in torsional angle space. In particular, we performed the calculation with the program DYANA,[19] with 300 random starting structures of the peptide and its metal complex and 10 000 steps of SA. Since only one molecule can be given as input in the program, the peptide was linked to Zn(II) through a long chain of linkers, i.e., residues made by atoms without van der Waals radii, which could freely rotate around their bonds, without causing steric repulsions, and thus enable one to sample a large number of relative positions of the ligand with respect to the metal ion before the minimization step.

Antimicrobial Activity. The antimicrobial activity was evaluated using seven different laboratory control strains of bacteria—Gram positive: *Staphylococcus aureus* (ATCC 25923), *Staphylococcus epidermidis* (ATCC 12228), *Micrococcus luteus* (ATCC 10240), *Enterococcus faecalis* (ATCC 29212). Gram negative: *Escherichia coli* (ATCC 25922), *Klebsiella pneumoniae* (NCIMB 9111), *Pseudomonas aeruginosa* (ATCC 27853). Two strains of yeast: *Candida albicans* (ATCC 24433) and *Candida albicans* (ATCC 10259). Active cultures for experiments were prepared by transferring a loopful of cells from the stock into tubes that contained 10 mL of Müeller-Hinton broth (MHB) for bacteria

(11) Brewer, D.; Lajoie, G. *Rapid Commun. Mass Spectrom.* **2000**, *14*, 1736–1745.
(12) Gusman, H.; Lendenmann, U.; Grogan, J.; Troxler, R. F.; Oppenheim, F.,G. *Biochim. Biophys. Acta* **2001**, *1545*, 86–95.
(13) Grogan, J.; McKnight, C. J.; Troxler, R. F.; Oppenheim, F. G. *FEBS Lett.* **2001**, *491*, 76–80.
(14) Kulon, K.; Valensin, D.; Kamysz, W.; Valensin, G.; Nadolski, P.; Porciatti, E.; Gaggelli, E.; Kozłowski, H. *J Inorg Biochem.* **2008**, *102*, 960–972.
(15) Fields, G. B.; Noble, R. L. *Int. J. Pept. Protein Res.* **1990**, *35*, 161–214.
(16) Christensen, T. *Acta Chem. Scand., Ser. B* **1979**, *33*, 763–776.
(17) Hwang, T. L.; Shaka, A. J. J. *J. Magn. Reson., Ser. A* **1995**, *112*, 275–279.
(18) Savitzky, A.; Golay, M. J. E. *Anal. Chem.* **1964**, *36*, 1627.
(19) Güntert, P.; Mumenthaler, C.; Wüthrich, K. *J. Mol. Biol.* **1997**, *273*, 283.

and Sabouraud dextrose broth (SDB) for fungi. After incubation for 24 h at 37 and 25 °C, the cultures were diluted with fresh Müeller-Hinton and Sabouraud dextrose broth in order to achieve optical densities corresponding to 2.5×10^6 colony forming units (CFU/mL) for bacteria and 1.2×10^7 CFU/mL for fungi and used as the inoculum.

Agar Diffusion Method. Müller-Hinton agar (MHA) and Sabouraud dextrose agar (SDA) (Institute for Immunology and Virology, Torlak, Belgrade) were used to test the sensitivity of bacteria and *C. albicans*, respectively. The MHA and SDA sterilized and cooled to 45−50 °C were distributed into sterile Petri dishes with a diameter of 9 cm to form a 4-mm-thick layer. The plates were inoculated with a previously prepared inoculum of bacteria or fungi in order to obtain semiconfluent growth. Prior to analysis, sterilized antibiotic discs (6 mm) were used following the literature procedure.[20] Fresh stock solutions of the compounds were prepared in dimethyl sulfoxide (DMSO) at a concentration of 1 mg/mL. The discs were impregnated with 20 μL of these solutions. To ensure that the solvent had no effect on microbial growth, a control test was performed with a test medium supplemented with DMSO. The discs injected with solutions were placed on the inoculated agar by pressing slightly and were incubated at 37 °C (24 h) for bacteria and 72 h at 26 °C for yeast *C. albicans*. On each plate, an appropriate reference antibiotic disk was applied, depending on the test microorganism. Reading of the results was carried out by measuring diameters of the inhibition zones in millimeters. In each case, triplicate tests were performed, and the average was taken as the final reading.

Ampicillin (10 μg/disk), amikacin (30 μg/disk), and nystatin (100 U/disk) served as positive controls.

Determinations of the Minimal Inhibitory Concentration (MIC). A broth microdilution method was used to determine minimal inhibitory bactericidal or fungicidal concentration (MIC) according to the National Committee for Clinical Laboratory Standards.[26]

All tests were performed in Müller-Hinton broth for bacterial strains and in Sabouraud dextrose broth for *Candida albicans*. Overnight, broth cultures of each strain were prepared, and the final concentration in each well was adjusted to 2.6×10^6 CFU/mL for bacteria and 1.2×10^7 CFU/mL for yeasts. The compounds were dissolved in 1% dimethylsulfoxide (DMSO) and then diluted to the highest concentration. Two-fold serial concentrations of the compounds were prepared (over the range of 62.5−1000 μg/mL) in a 96-well microtiter plate. In the tests, triphenyl tetrazolium chloride (TTC; Aldrich Chemical Co., Inc., U. S. A.) was also added to the culture medium as a growth indicator. The final concentration of TTC after inoculation was 0.05%. The microbial growth was determined by absorbance at 600 nm using a universal microplate reader after incubation at 37 °C for 24 h for bacteria and at 26 °C for 48 h for fungi. The MIC is defined as the lowest concentration of the compound at which the microorganisms do not demonstrate visible growth. All determinations were performed in triplicate, and two positive growth controls were included.

Results

Metal-Free P113. NMR studies were performed in water as well as in DMSO solutions, with P113 and its N-acetylated parent peptide (AcP113) displaying very similar NMR spectra. At $T = 298$ K and pH = 7.0, most of the amide proton signals were extensively broadened in water; however, lowering the temperature to 278 K resulted in sharper NMR signals (Figure 1S, Supporting Information). On the contrary, all amide protons were easily detectable in DMSO in the temperature range 298−318 K (data not shown). The full assignment in both solvents (Tables 1S, Supporting Information) was accomplished using ^{1}H−^{1}H TOCSY, NOESY, and ROESY spectra. These last experiments additionally revealed the absence of any "not-trivial" NOE cross-peaks, indicating that P113 assumes a disordered structure in both solvents, as also verified by the intense negative absorption at 196 nm in CD, typical of the random coil conformation[21] (Figure 2S, Supporting Information).

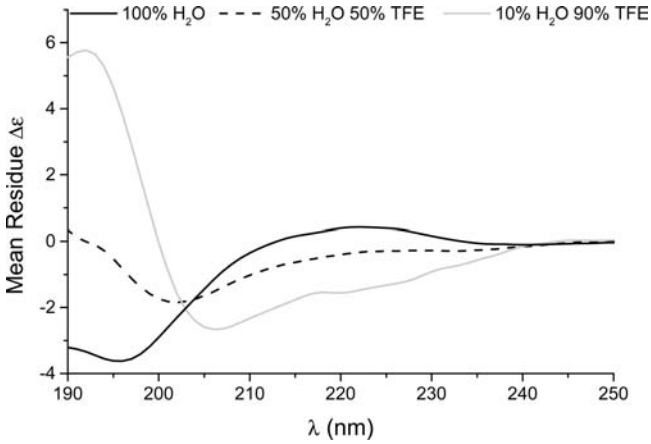

Figure 1. CD spectra of P113 in water (black solid line) and in the presence of different TFE percentages: 50% TFE (black dash line) or 90% TFE (solid gray line). All of the samples were at pH 7.0, $T = 298$.

Since it has been suggested that the antimicrobial activity of histatins[22,23] and P113[4] is related to their propensity to form helical structures, the behavior of P113 in TFE−water mixtures was also investigated. Figure 1 shows that the CD spectra of P113 are strongly affected by TFE:

(i) At 50% TFE, the intensity of the band at 196 nm is decreased, and it is shifted to 205 nm.

(ii) At 90% TFE, the CD signal is strongly modified, and two negative band centered at 208 and 225 nm are visible.These absorptions are typical of an α helix conformation[21] and are in agreement with previously recorded data.[4]

NMR spectra of P113 in TFE-D_2O (9:1) solutions at pH 7 were obtained as well. The obtained spectra showed the presence of very weak amide signals at both 298 and 278 K, thus preventing the structure determination. However, Hα protons were all showing negative CSI (Chemical Shift Index) deviations from the random coil chemical shift values, suggesting the occurrence of an α helix conformation (Figure 2).

The high antimicrobial activity of P113 against clinical isolates of *C. albicans* was previously reported.[4] The various clinical isolates were all found to be sensitive to 3.1 μg/mL of P113.[4] In this study, the antimicrobial activity of P113 and AcP113 against nine different laboratory

(20) *NCCLS 2001* (*National Committee for Clinical Laboratory Standards*), *Performance Standards for Antimicrobial Susceptibility Testing, 11th informational supplement, Document M100−S11*; National Committee for Clinical Laboratory Standard: Wayne, PA, 2001.

(21) Greenfield, N. J.; Fasman, G. D. *Biochemistry* **1969**, *8*, 4108–4116.
(22) Raj, P. A.; Soni, S. D.; Levine, M. J. *J. Biol. Chem.* **1994**, *269*, 9610–9619.
(23) Ramalingam, K. T.; Gururaja, L.; Ramasubbu, N.; Levine, M. J. *Biochem. Biophys. Res. Commun.* **1996**, *225*, 47–53.

control strains of microorganisms was determined as well. In particular, both the agar diffusion and broth microdilution methods were used. The results of the broth microdilution method agree with those of the agar diffusion one as for the activity against *C. albicans*. The obtained MIC values for both P113 and AcP113 are reported in Table 1. The highest activity was found for P113, which shows MIC values of 32 μg/mL for both strains of *C. albicans*. The obtained MIC values are 10 times smaller than the previously reported one, probably due to the use of different methods.[4]

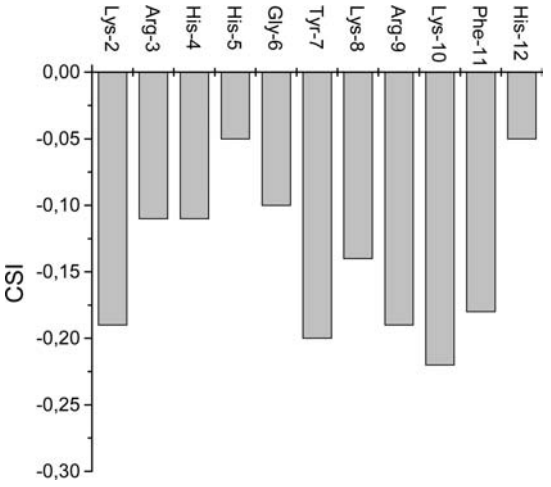

Figure 2. CSI of the Hα signal of P113, 0.5 mM , 90% TFE−10% H_2O, pH 7.

Zn(II)−P113 Complex. The effects of adding Zn(II) to P113 and AcP113 solutions were evaluated using CD and NMR. Three different environments were studied: (i) 100% DMSO, (ii) 100% H_2O, and (iii) 90% TFE−10% H_2O (or D_2O). The obtained results are independently reported for each system.

DMSO Solutions. The addition of Zn(II) determined significant line broadening and changes in the chemical shift of several ^{1}H signals of both P113 and AcP113 (Figures 3S and 4S, Supporting Information). Zinc titrations revealed that up to 6.0 Zn(II) equivalents were necessary to reach the chemical shift "plateau" for both P113 and AcP113. The most affected signals were the His aromatic protons and the Gly-6 NH, as verified by the calculated $\Delta\delta$ values (Figure 3). As a whole, the effects of Zn(II) can be summarized as follows:

(i) Shifts experienced by His aromatic resonances are revealing for the involvement of the imidazole rings in Zn(II) coordination; moreover, all His Hε being more affected than Hδ (Figures 3 and 3S), Zn(II) binding to His-4, His-5, and His-12 Nδ can be suggested.

(ii) The strong perturbation on Gly-6 NH (shifted 0.40 ppm upfield in both complexes) suggests some structural rearrangement brought about by Zn(II) binding.

(iii) The effects monitored on the N-terminal region in P113 only, Ala-1, Lys-2, and Arg-3 protons

Table 1. Minimal Inhibitory Concentration (MIC in μg/mL) of Tested Compounds

microorganism	P113	Ac−P113	Zn−P113	Cu−P113	ampicillin	amikacin	nystatin
S. aureus	75.0	32.5	250	250	1.0	2.0	n.t.
S. epidermidis	75.0	32.5	500	250	n.t.	n.t.	n.t.
M. luteus	16.0	75.0	250	250	n.t.	n.t.	n.t.
E. faecalis	16.0	16.0	250	250	2.0	n.t.	n.t.
E. coli	250	> 500	> 500	> 500	8.0	4.0	n.t.
K. pneumoniae	250	> 500	> 500	> 500	n.t.	n.t.	n.t.
P. aeruginosa	> 500	> 500	> 500	> 500	n.t.	2.0	n.t.
C. albicans (ATCC 10259)	32.5	75.0	500	> 500	n.t.	n.t.	3.0
C. albicans (ATCC 24433)	32.5	75.0	500	> 500	n.t.	n.t.	4.0

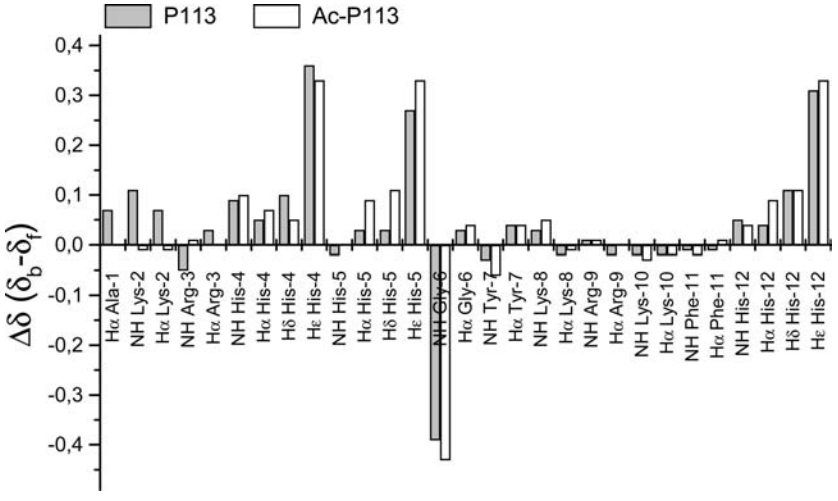

Figure 3. Zn(II)-induced chemical shift variations ($\Delta\delta$) on P113 (white bars) and on Ac−P113 (gray bars) protons. Both peptides were in DMSO, T = 318 K.

Table 2. Temperature Coefficients (ppb/K) of All NH's of the Zn(II)−P113 complex, pH = 7.0, DMSO

amino acid	δ/T ppb/K
Ala-1	n.d
Lys-2	n.d
Arg-3	-9.5_5
His-4	−5.3
His-5	−5.7
Gly-6	−2.9
Tyr-7	−5.4
Lys-8	−6.9
Arg-9	−5.2
Lys-10	−4.3
Phe-11	−5.3
His-12	−5.7

being shifted upon metal addition (Figures 3 and Figure 3S, Supporting Information), indicate the additional involvement of Ala-1 NH_2 in the P113−Zn(II) system.

(iv) $^1H-^1H$ TOCSY spectra of AcP113−Zn(II) disclose intense cross-peaks for both the Arg-3 and Arg-9 side chain NH_ε's that were not detectable in the free Ac-P113 (Figure 4S, Supporting Information); on the contrary, between the two weak Arg-3 and Arg-9 NH_ε cross-peaks detectable in the $^1H-^1H$ TOCSY spectra of free P113 (at 7.67 and 7.53 ppm, respectively), the one belonging to Arg-3 is shifted by Zn(II) (Figure 4S, Supporting Information), thus ratifying the additional involvement of the Ala-1 amine group in the Zn(II)−P113 complex.

Further information was gained by measuring the temperature dependence of the chemical shift of amide protons in the range 298−328 K. The obtained temperature coefficients (Table 2) are consistent with Gly-6 being involved in intramolecular hydrogen bonding, which can easily explain the large chemical shift perturbation experienced by Gly-6 upon Zn(II) addition.

The 3D structures of P113−Zn(II) and AcP113−Zn(II) complexes were obtained by $^1H-^1H$ NOESY spectra analysis. Though not showing any correlation typical of definite secondary structures, all of the cross-peak integrals allowed for obtaining a set of proton−proton distances to be used as restraints in structural calculations. The first 11 structures obtained for the P113−Zn(II) and AcP113−Zn(II) complexes are reported in Figure 4. Both structure families were fitted on the coordination site. The P113−Zn(II) structures possessed a target function in the range of 0.012−0.024, and the calculated RMSD was 0.04 ± 0.01 and 0.15 ± 0.04 nm, respectively, for the backbone and for the heavy atoms. The structures of the P113 complexes (Figure 4A) were characterized by a well fitted N-terminus, residues 1−5, and a less defined C-terminus, the 6−11 region being very spread as a consequence of the shortage of restraints in the input files. In fact, Lys-8, Arg-9, and Lys-10 spin systems were extensively overlapped, such that unequivocal assignment of cross peaks in the NOESY spectra was precluded. In the Ac−P113−Zn(II) structures, reported in Figure 4B, two distinct regions are observed as well:

(i) A disordered N-terminus, not involved in the coordination of the metal

(ii) A well-defined binding region encompassing residues 4−12. The target function is in the range of 0.14−0.19, and the calculated RMSD is 0.02 ± 0.01 and 0.09 ± 0.02 nm, respectively, for the backbone and for the heavy atoms.

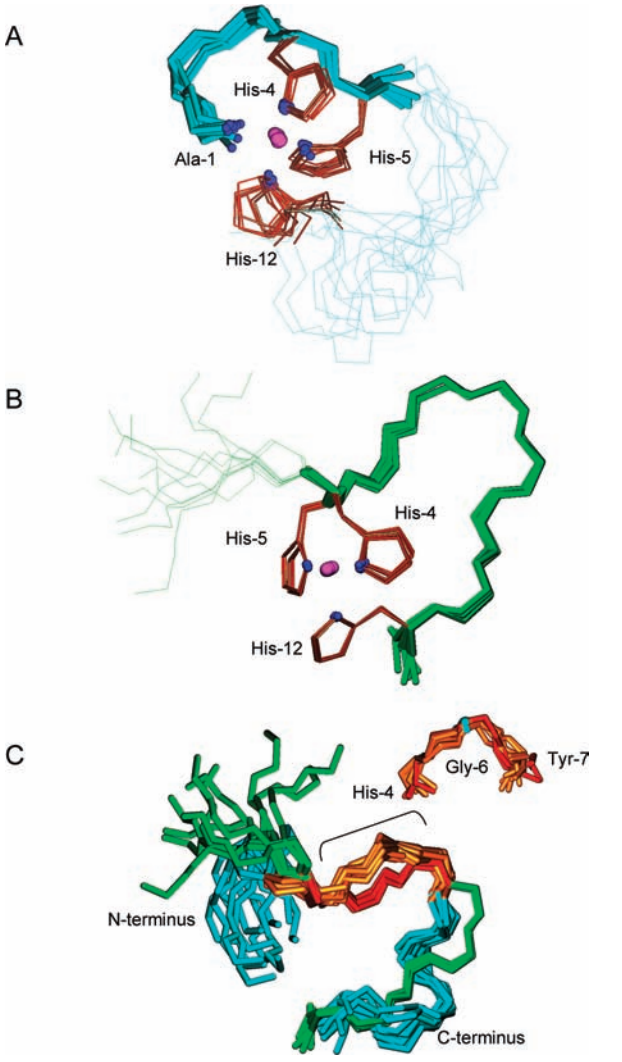

Figure 4. Structures obtained from NOESY spectra in DMSO. (A) The first 11 structures obtained for the P113−Zn(II) complex. The nitrogen donor atoms of Ala-1, His-4, His-5, and His-12 are shown as blue spheres. The Zn(II) ion is shown as a magenta sphere. The structures are fitted on the backbone of residues 1−5. (B) The first 11 structures obtained for the Ac−P113−Zn(II) complex. The nitrogen donor atoms of His-4, His-5, and His-12 are shown as blue spheres. The Zn(II) ion is shown as a magenta sphere. The structures are fitted on the backbone of residues 4−12. (C) Comparison of the structures obtained for P113 (cyan) and Ac−P113 (green) complexes. The structures are fitted on the backbone of residues 4−12. The most similar part comprises residues 4−7. In the inset are shown the 4−7 backbone of P113 (orange) and Ac−P113 (red) complexes when fitted on 4−7 residues only. The Gly N_H is shown as a cyan sphere. This figure was created with MOLMOL 2K.1.0.

Aqueous Solutions. Water solutions of P113 at T = 278 K were titrated with the Zn(II) ion. Adding the metal was accompanied by the appearance of new NMR signals and the simultaneous disappearance of the old ones (Figure 5S, Supporting Information). Up to 2.0 Zn(II) equivalents were required to exclusively observe the metal-bound form. The presence of Zn(II) also caused consistent line broadening of most of the amide protons, which had almost vanished after the addition of 1.0 metal equivalent.

The calculated ^{13}C and ^{1}H changes in chemical shift, reported in Figure 5, are consistent with metal binding to His imidazoles and to the amino terminal group. Moreover, the NOESY spectra revealed the existence of "not trivial" inter-residue dipolar correlations that give evidence of spatial proximity between His aromatic protons (Hδ and Hε) and Ala-1, Lys-2, and Tyr-7 aliphatic protons (Figure 6).

Distance restraints, obtained by the volumes of NOE cross-peaks, allowed determination of the 3D structure of the metal complex in water. The first 12 structures, reported in Figure 7, were fitted in the region encompassing residues 1−6. The obtained structures possessed a target function in the range of 0.50−0.58, and the calculated RMSD was 0.01 ± 0.01 and 0.09 ± 0.03 nm, respectively, for the backbone and for the heavy atoms. As pointed out by the very low RMSD values, the structures are well

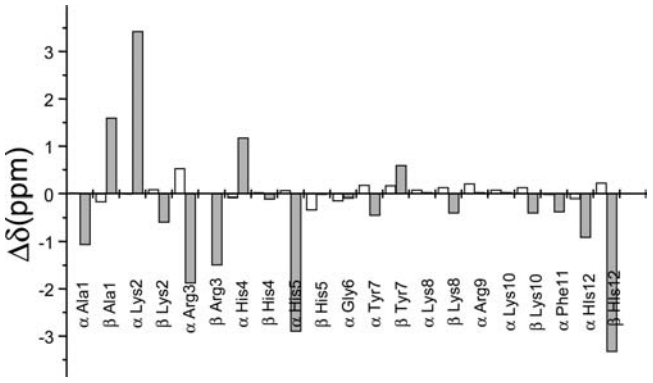

Figure 5. Zn(II)-induced chemical shift variations (Δδ) on P113 ^{1}H (white bars) and ^{13}C signal (gray bars) protons. P113 was in water, pH 7.0, T = 278 K.

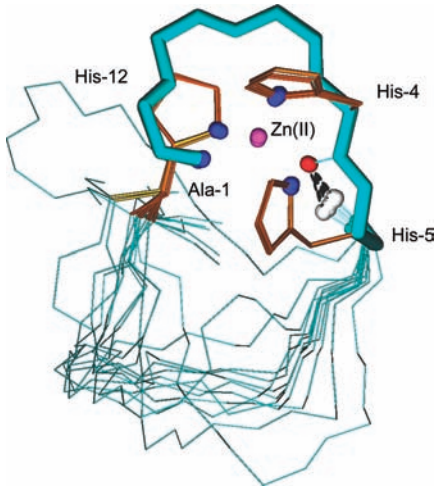

Figure 7. Structures obtained from NOESY spectra in H_2O. (A) The first 11 structures obtained for the P113−Zn(II) complex . The nitrogen donor atoms of Ala-1, His-4, His-5, and His-12 are shown as blue spheres. His-4 carbonyl O and Gly NH are shown as red and with a sphere, respectively. The Zn(II) ion is shown as a magenta sphere. The structures are fitted on the backbone of residues 1−5. This figure was created with MOLMOL 2K.1.0.

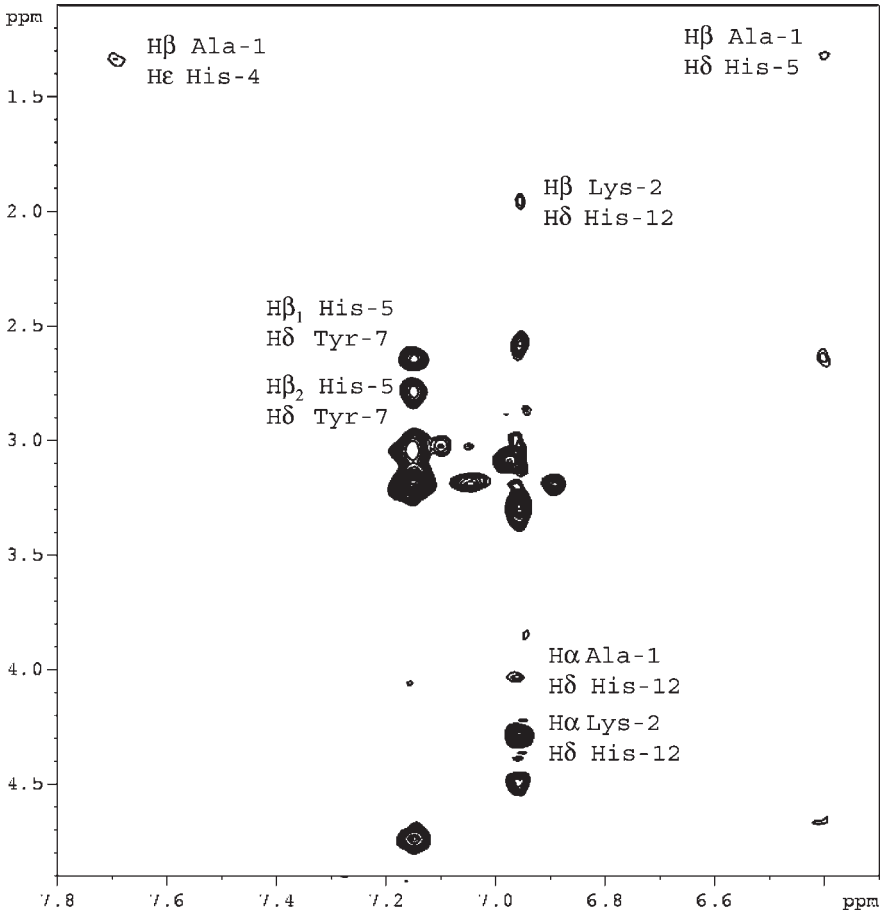

Figure 6. Selected region of $^{1}H-^{1}H$ NOESY NMR spectra of P113 1.0 mM, pH 7.0, T = 278 K in water and in the presence of 3.0 equiv of Zn(II).

Table 3. Antimicrobial Activity (Zone of Inhibition in millimeters)

microorganism	P113	Ac−P113	Zn−P113	Cu−P113	ampicillin	amikacin	nystatin
S. aureus	0	0	0	0	35.0	23.0	n.t.
S. epidermidis	0	0	0	0	20.0	n.t.	n.t.
M. luteus	0	0	0	0	33.0	n.t.	n.t.
E. faecalis	0	0	9.0	8.0	16.0	n.t.	n.t.
E. coli	0	0	8.0	8.3	21.0	20.0	n.t.
K. pneumoniae	0	0	7.7	7.3	17.0	n.t.	n.t.
P. aeruginosa	0	0	8.5	9.3	10.0	27.5	n.t.
C. albicans (ATCC 10259)	12.0	0	13.3	13.7	n.t.	n.t.	21.0
C. albicans (ATCC 24433)	11.0	0	8.3	8.3	n.t.	n.t.	21.0

superimposed in the N-terminal metal binding region; whereas, although the His-12 side chain is nicely defined, residues far away from the metal binding sites are very spread. Interestingly, all the reported structures are characterized by the occurrence of a hydrogen bond between Gly-6 NH and His-4 CO (Figure 7).

CD spectroscopy was additionally used to look at Zn-induced conformational changes of P113 in water. CD absorptions in the 191−250 nm wavelength region were detected for P113 in the presence of Zn(II) at pH 7.0. A strong Zn(II)-induced reduction of the absorption at 196 nm was apparent (Figure 1S, Supporting Information), supporting the view that the metal favors some structural rearrangement.

The antimicrobial activity of Zn(II) complexes was tested together with that of Cu(II) adducts, since Cu(II) has been reported to display high binding affinity for P113.[14] The two metal complexes were behaving in a very similar fashion (Tables 1 and 3), suggesting a possible similar role. We found that both metal complexes exhibited a lower activity (MIC values for Zn−complex were 500 μg/mL for both strains of *C. albicans*) than that of the metal-free P113 (MIC values for P113 were 32 μg/mL for both strains of *C. albicans*) as shown in Table 1. The metal complexes' activity toward other bacteria was tested as well. Generally, the Gram-negative bacteria were less sensitive than the Gram-positive ones (Table 3), and among these, *Enterococcus faecalis* and *Micrococcus luteus* were the most sensitive (MIC values of the tested compounds 250 μg/mL; Table 1). Both Zn(II) and Cu(II) complexes exhibited MIC values higher than those of the free ligand, contrary to what was previously reported for histidine-rich peptides,[13] where Zn(II) was proposed to regulate their antimicrobial activities against *Enterococcus faecalis*.

TFE−Water Solutions. No definite information could unfortunately be extracted from NMR data because

(i) The presence of Zn(II) caused severe line broadening of most NMR resonances

(ii) The suppression of the H_2O signal, located at 3.9 ppm, determined the simultaneous disappearance of signals nearby

(iii) Many signals belonging to the amide protons could not be observed even in the free ligand-Nevertheless, CD spectroscopy allowed for monitoring of the structural rearrangements of P113 upon Zn(II) binding. Figure 8A and B report the effects of Zn(II) for solutions containing 50% and 90% of TFE, respectively. In both cases, the CD absorptions of the metal complex were significantly different from those of free P113, suggesting that Zn(II) binding is accompanied by structural transitions of the peptide. In particular, the spectra recorded at 90% TFE showed an extensive decrease in the intensities of the negative bands centered at 205 and 220 nm, strongly indicating a high reduction of α helix content.

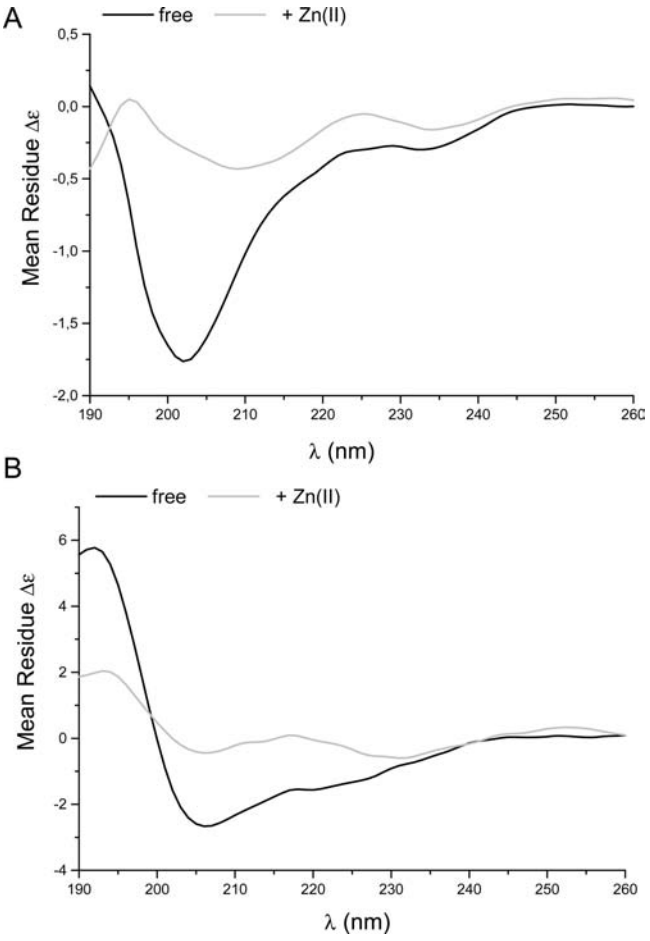

Figure 8. CD spectra of P113, 0.10 mM, pH 7, in a water−TFE mixture in the absence (black) and in the presence of Zn(II) (gray). (A) 50% TFE. (B) 90% TFE.

Discussion

P113, a derivative of Hsn-5, having potent *in vitro* activity against the major *Candida* pathogens,[4] has been reported to form a stable complex with copper(II),[14] in which the His−His pair and the N-terminal group act as the main Cu(II) anchoring sites. In the present work, Zn(II) binding was considered, and the Zn(II)−P113 complex was characterized. Moreover, eventual metal-induced modifications of the antimicrobial activity of P113 were sought in order to assess whether Zn(II) and/or Cu(II) may be effective in modulating the biological actions of P113 *in vivo*.

Zn(II)-binding equilibria were approached by solution NMR and CD studies. Structural features were searched in three different solvents, namely, DMSO, water, and water−TFE mixtures, in order to optimize the experimental setting and possibly verify the stabilizing role of the solvent. CD spectra were obtained in water or water−TFE solutions only, due to the masking intense CD signals of DMSO in the used wavelength range. In any case, NMR and CD spectra were consistent with P113 being devoid of structural elements in water or DMSO; whereas an α-helix conformation was given evidence in the presence of a high TFE percentage.

The flexible and disordered nature of P113 in solution makes NMR detection of amide protons essential for the assignment. In fact, extensive overlapping occurs within the aliphatic region that hopelessly hampers the usual ways that information is gained: the spin systems of the three Lys and the two Arg residues are completely merged together, as occurs for the spin systems of Tyr-7, Phe-11, and the three His residues. From this point of view, substantial improvement is offered by DMSO solutions where all amide protons are NMR-detectable at room as well as higher temperatures. On the contrary, the detection of weak NH signals in water or TFE−water mixtures is only possible when lowering the temperature to 278 K. These are the reasons why NMR experiments were mainly performed at 318 K in DMSO and at 278 K in water or water−TFE, although, as already stated, no NMR restraints could be determined in the latter case.

Metal binding domains and metal-induced structural modifications were mainly obtained by looking at the effects of Zn(II) upon NMR parameters; the addition of Zn(II) entails extensive and selective broadening and chemical shift variations of several proton resonances. In DMSO or in water, the largest effects involve all three His's (Figures 3 and 5), strongly indicating Zn(II) binding to the imidazole rings of His-4, His-5, and His-12 with the additional involvement of Ala-1 NH_2, as ratified by the $\Delta\delta$ values recorded on the N-terminus residues (Figures 3 and 5), within the Zn(II)−P113 system.

NMR NOESY maps provided the input parameters for delineating the 3D structures of Zn(II)−P113 in DMSO (Figure 4A) and in water (Figure 7). The two families of structures are compared in Figure 9, where a nice superimposition of metal binding regions (residues 1−5) is apparent and ratified by the RMSD values, which are 0.06 ± 0.04 and 0.19 ± 0.08 nm, respectively, for the backbone and for the heavy atoms. Moreover, the temperature coefficients calculated in DMSO solution and the detection of inter-residue hydrogen bonds in the structure of Zn(II)−P113 (Figure 7) strongly imply Gly-6 NH being engaged in intramolecular hydrogen bonding, thus explaining the corresponding large chemical shift variations detected in Figure 3.

The detected chemical shift variations shown by Lys-2 and Arg-3 residues (Figures 3 and 5, Figures 3S and 4S, Supporting Information) are consistent not only with metal binding to the N-terminal amino group but also with the peptide region encompassing residues 1−5 assuming a well-defined structure (Figures 4 and 7). The fact that the C-terminus of the peptide is relatively mobile and undefined in the metal complexes supports the view that coordination to His-12 only plays a minor role in the zinc-induced structural rearrangement, as also found in the case of the P113−Cu(II) complexes.[14]

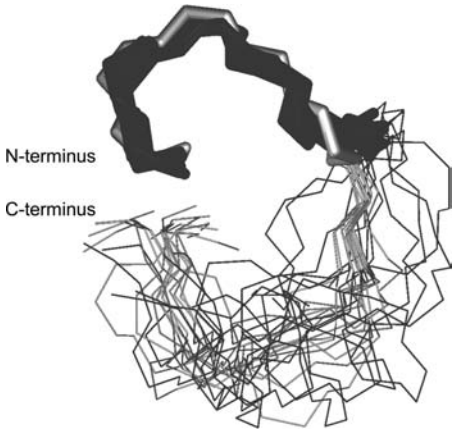

Figure 9. Superimposition of the best 11 structures of Zn(II)−P113 obtained from experimental data recorded either in DMSO-d6 (black) or in water (light gray). This figure was created with MOLMOL 2K.1.0.

The comparison between the structures of Zn(II)−P113 and Zn(II)−Ac-P113 (Figure 4C) is revealing for the structural role played by the N-terminal group that is expected to strongly modify the metal coordination sphere and, consequently, the conformation of the peptide. Figure 4C shows that the regions encompassing residues 4−12, containing the three His's involved in metal binding, have completely different folding, with the exception of just the backbone region containing His-4, His-5, Gly-6, and Tyr-7 (*inset*); these common features can explain why the Gly-6 NH experiences very similar chemical shift variations in the two metal complexes (Figure 3).

Present and previous findings agree in designating P113 a good ligand for both Zn(II) and Cu(II),[14] with the three His imidazoles and the N-terminal amino acting as the binding donors for both metal ions and with the His−His pair playing a major role in stabilizing the complex. A comparison between the structures of the two metal complexes shows that Cu(II)−P113[14] is better defined, all three His side chains being precisely located (Figure 6S, Supporting Information). Although they share the same metal donor domains, the two complexes assume different conformations as a consequence of the different geometries of the coordination sphere, that is, in tetrahedral and tetragonal arrangements for Zn(II) and Cu(II), respectively.

As for the antimicrobial activities, Zn(II)−P113 and Cu(II)−P113 were shown to behave rather similarly. Present and previous findings[4] agree in assessing that P113 exhibits the best activity against yeast *C. albicans*, the major fungal pathogen in humans. However, binding of Zn(II) or Cu(II) yields higher MIC values compared with those observed with free P113. Also nystatin, used as a control in the antimicrobial activity studies, shows higher activity than both metal complexes. Since copper and zinc metal complexes have different arrangements, the low activity exhibited by the metal-bound P113 is better ascribed to the absence of an α-helix conformation rather than to specific effects of the metals. In fact, metal binding to the N-terminal group, to the His−His pair, and to the last His makes the peptide less prone to form α-helix structure elements, already shown to be crucial for antimicrobial activities of P113 and histatin.[4,22,23] In support of this view, the CD spectra of P113 in TFE/water (9:1) verify the reduction in α helix content upon Zn(II) binding (Figure 8).

The negative effects played by the metal ions may be relevant if we consider that P113 can be effectively bound by Zn(II) *in vivo*. In fact, zinc is the second most abundant trace element in the body, is essential for eukaryotic and prokaryotic organisms, and is required as a cofactor or structural component for more than 100 metalloenzymes in all six classes of enzymes.[24,25] Fungal infections have become increasingly significant as a consequence of the growing population of immunocompromised patients. For example, up to 46% of AIDS patients experience symptoms of oral candidiasis.[26] The emergence of resistant fungal pathogens has been a motivating force in the search for new antifungal agents. Antimicrobial peptides, including histatins, have been considered prime candidates because they probably have a mode of action distinct from those of other antifungal agents[32,27] However, our findings suggest that metal binding to P113 or similar antimicrobial peptides dramatically reduced their antimicrobial activity *in vitro*, suggesting a possible role played by Zn(II) *in vivo* as well.

Acknowledgment. We thank the CIRMMP (Consorzio Interuniversitario Risonanze Magnetiche di Metalloproteine Paramagnetiche) for financial support.

Supporting Information Available: ^{1}H NMR chemical shift of apo P-113 and Ac-P-113 (Table 1S). ^{1}H 1D spectra of P-113 water at T = 278 and T = 298 K (Figure 1S); CD spectra of P-113 in the absence and in the presence of 3.0 or 6.0 Zn(II) eqs (Figure 2S). Selected regions of ^{1}H 1D NMR spectra of P-113 and AcP113 in DMSO-d_6 at T = 318 K in the absence and in the presence of Zn(II) (Figure 3S). Selected regions of ^{1}H$-^1$H TOCSY spectra of P-113 and AcP113 in DMSO-d_6 in the absence and in the presence of 6.0 Zn(II) eqs (Figure 4S). Selected regions of ^{1}H 1D NMR spectra at T = 278 K of P-113 in the presence of different amounts of Zn(II) (S). Comparison of the Zn(II)-P113 and Cu(II)-P113 structures (Figure 6S). This material is available free of charge via the Internet at http://pubs.acs.org.

(24) Broadley, M. R.; White, P. J.; Hammond, J. P.; Zelko, I.; Lux, A. *New Phytologist* **2007**, *173*, 677.

(25) *Dietary Reference Intakes for Vitamin A, Vitamin K, Arsenic, Boron, Chromium, Copper, Iodine, Iron, Manganese, Molybdenum, Nickel, Silicon, Vanadium, and Zinc*; United States National Research Council, Institute of Medicine; National Academies Press: Washington, DC, 2000.

(26) White, T. C.; Marr, K. A.; Bowden, R. A. *Clin. Microbiol Rev*. **1998**, *11*, 382–402.

(27) De Lucca, A. J.; Walsh, T. J. *Antimicrob. Agents Chemother*. **1999**, *43*, 1–11.